Shakedown analysis of modified Bree problems involving thermal membrane stress and generalized loading conditions

Hongchen Bao[1], Jun Shen[1], Yinghua Liu[1*], Haofeng Chen[2*]

1. Department of Engineering Mechanics, AML, Tsinghua University, Beijing, 100084, China
2. Department of Mechanical and Aerospace Engineering, University of Strathclyde, 75 Montrose Street, Glasgow G1 1XJ, Scotland, United Kingdom

Abstract:

For industrial components such as pressure vessels and piping systems, it is important to determine the shakedown domains of structures under complex variable thermo-mechanical loads to avoid low cycle fatigue due to alternating plasticity or incremental plastic collapse caused by ratcheting. In this paper, the interaction among three common types of stresses are considered based on a plane model, namely, mechanical membrane stress, thermal membrane stress and thermal bending stress. Strict shakedown analysis is performed based on the Linear Matching Method under multiple variable mechanical and thermal loads. Three-dimensional shakedown domains for three types of modified Bree problems involving thermal membrane stress and generalized loading conditions are given for the first time, and the three-dimensional shakedown boundaries are expressed as two-dimensional parametric equations by introducing a new parameter called "secondary membrane bending ratio" *R*. By comparing the 3S criterion plane with the newly obtained 3D shakedown boundaries, the conservatism and non-conservatism of the 3S criterion are discussed under different loading paths. As an extension of the 3S criterion, a new and economical criterion on elastic shakedown assessment is proposed for generalized thermo-mechanical loading. The proposed shakedown boundary parametric equations and shakedown checking method can provide guidance for engineering design and safety assessment.

***Keywords*:** Elastic shakedown, Two-plane model, Linear Matching Method, 3S criterion, Thermal membrane and bending stress

1. Introduction

Pressure vessels are key equipments in process industry, and they are widely used in nuclear energy, petroleum, chemical, electric power, pharmaceutical and other fields. With the development of industrial equipments towards large-scale and high-parameter, the service conditions for many structural elements are more and more harsh. Many practical structural components including cracking furnaces, high-temperature boilers, industrial pipelines, nuclear reactors and piping systems have some common characteristics: they are all in service under high temperature environment, and are all subjected to complicated cyclic or changing thermo-mechanical loads due to start-up and shutdown. In order to protect structures from alternating plasticity or ratcheting, it is necessary to determine the shakedown boundaries of these structures under cyclic loading, so as to provide accurate and reliable basis for engineering design and safety assessment.

The Bree diagram[1-2] is often used to show the different stress regimes of structure under cyclic thermal load and constant internal pressure, and it is also the theoretical basis of the shakedown design criterion of pressure equipment in the ASME code. Bree problem considers the shakedown and ratcheting behaviors of an axisymmetric cylindrical shell under the interaction of constant mechanical membrane stress and cyclic thermal bending stress. The basic assumption of the classical Bree problem is that the action section of stress does not allow rotation, and only the radial thermal stress is considered in the secondary stress. In 2005, Kalnins[3] studied the ratcheting behavior of a cylinder considering the interaction between radial (or axial) thermal gradient and internal pressure through finite element elastic-plastic analysis. It was found that when the thermal membrane stress induced by axial thermal gradient was dominant in the thermal stress, Bree ratcheting boundary and 3S criterion were not conservative. In 2008, Reinhardt[4] considered the interaction between constant mechanical membrane stress, cyclic thermal bending stress and thermal membrane stress in shakedown analysis, and established three-dimensional ratcheting boundary by non-cyclic method. Based on his theoretical derivation and simplified recommendations, ASME VIII-2 2013 edition[5] made slight modifications to checking rules for thermal stress ratcheting, where a limit on the thermal membrane stress range was added, and "thermal bending stress" was replaced with "thermal stress" in the simplified elastic-plastic analysis. Asadkarami et al[6] studied the influence

Contact author email:[1] yhliu@tsinghua.edu.cn, [2] haofeng.chen@strath.ac.uk

of thermal discontinuity involving thermal membrane and thermal bending stress on shakedown boundary.

Compared with the Bree problem, one more type of stress is considered in Reinhardt's work, that is, the thermal membrane stress. However, the interaction between primary bending stress and other types of stresses is not considered. In 2018, Shen et al[7] broke the limitation on the basic assumption of section translation deformation, and developed a new ratcheting boundary theory considering the interaction among four types of stresses, i.e., constant mechanical membrane stress, mechanical bending stress, cyclic thermal membrane stress, and thermal bending stress. Two more types of stresses are considered in Shen's work compared with the original Bree problem, and the unified ratcheting boundary given by Shen can be degenerated to the Bree problem and the inverse Bree problem. A novel two-plane model was also proposed to simulate accurately the interaction among the four types of stresses simultaneously, which can not be handled by the previous models.

From the work of Bree[1], Reinhardt[4] and Shen[7], it can be found that the types of stresses considered in the ratcheting theory have been increased, and the applicable scope of ratcheting checking is extended from the location far away from the structural discontinuity to the gross structural discontinuity area. However, their theoretical derivations are only limited to a simple loading condition, that is, the mechanical load remains constant and the thermal load keeps cycle. For Bree-type ratcheting and shakedown problems considering two types of stresses, many theoretical and numerical studies have been reported. For instance, Moreton et al [8] in the 1980s, and Bradford[9-10] in recent years had both independently derived the in-phase and out-of-phase modified Bree diagrams by modifying the loading condition in the original Bree problem[11]. Pei and Dong[12-13] developed a universal approach for Bree-type ratcheting problems, which can automatically generate a series of Bree-like diagrams considering arbitrary loading and material nonlinearity conditions. Peng et al.[14] studied three types of Bree shakedown problems numerically using the stress compensation method. As for modified Bree problems involving three or four types of stresses under complex loading cases, the relevant research is rarely reported. Since multiple types of stresses are considered in the elastic stress ratcheting analysis method of the ASME code, it is necessary to further study the shakedown and ratcheting boundaries considering the interaction of multiple stresses under complex thermo-mechanical loads.

Currently, the ASME VIII-2 2019 edition[15] provides two kinds of ratcheting assessment methods: the elastic stress ratcheting analysis method (paragraph 5.5.6) and the elastic-plastic stress ratcheting analysis method (paragraph 5.5.7), but there is no shakedown assessment method. The only rule that can be used for elastic shakedown analysis is the elastic ratcheting analysis method, i.e., the 3S criterion. However, the 3S criterion does not represent a complete elastic shakedown boundary in most cases, fulfillment of this criterion does not ensure elastic shakedown generally. Recently, Shen et al.[16] proposed a complete elastic ratcheting assessment method that can be used to prevent the loss of elastic shakedown based on the 3S criterion and supplementary assessment of thermal stress ratcheting. Since the checking rule of thermal stress ratcheting is actually based on the simplified representation of the Reinhardt ratcheting boundary, it is very conservative to use the restriction on thermal stress ratcheting to supplement the 3S criterion.

For the shakedown analysis considering complex loading cases, the step-wise analytical derivation is very cumbersome and error prone. For example, Moreton and Ng[17-19] published several articles in the 1980s to correct some oversights made in their original derivations [8]. Since the governing equations of the modified Bree problems involving three or four types of stresses are very complicated, the theoretical derivation under more complex loading conditions is very difficult. For actual engineering structural components in operation, the loading conditions cannot be changed arbitrarily, and the cost of experimental research is very high. With the development of computer technology and numerical algorithm, finite element simulation provides a powerful tool for shakedown problems. By means of numerical analysis, the shakedown boundary considering multiple types of stresses interaction can be obtained under arbitrary loading cases. Since the step-by-step analysis method needs a lot of trial calculation to obtain the shakedown limit, the accurate and efficient direct method (such as the Linear Matching Method[20-21], LMM) has more advantages in constructing the shakedown and ratcheting boundaries.

The objective of this paper is to study the modified Bree shakedown problems involving thermal membrane stress and generalized loading conditions numerically, and to develop a new and economical elastic shakedown assessment method based on the complete shakedown boundaries and the corresponding parametric equations. The article is outlined as follows. Section 2 presents the numerical procedure for strict shakedown analysis based on the LMM. The two-plane model is introduced in Section 3. Three types of modified Bree problems are analyzed systematically in Section 4. Then a new and economical elastic shakedown evaluation criterion is proposed in Section 5. Finally, some key conclusions are given in Section 6.

2. Numerical procedure for shakedown analysis based on the LMM

The LMM is a fast and direct method for solving the responses of various complex structures considering non-linear material properties under arbitrary thermal-mechanical load combination, which consists of a series of linear elastic analyses with modified elastic modulus to simulate the structural plastic behavior[22-23]. The robustness and applicability of the LMM has been verified by FE step-by-step analysis. Through solving a series of classical problems and complex engineering examples, it is shown that the LMM is capable of calculating shakedown and ratcheting boundaries accurately and efficiently[24-25]. The brief introduction of the numerical procedures for strict shakedown analysis in the LMM is given below.

2.1 **Cyclic plasticity problem**

For a structure body with volume V and surface S, assume that it is subjected to a varying thermal load $\lambda_\theta \theta(x,t)$ in the volume V, and a varying mechanical load $\lambda_P P(x,t)$ acts on surface S_t, zero-displacement boundary condition is satisfied on surface S_u (=S-S_t), where the change of thermal load and mechanical load has the same period T. For the time history in a cycle $0 \leq t \leq \Delta t$, the linear elastic stress solution of the structure body can be expressed as:

$$\hat{\sigma}_{ij}(x,t) = \lambda_p \hat{\sigma}_{ij}^{P}(x,t) + \lambda_\theta \hat{\sigma}_{ij}^{\theta}(x,t) \tag{1}$$

where $\hat{\sigma}_{ij}^{P}(x,t)$ denotes the linear elastic solution of pure mechanical load $P(x,t)$, $\hat{\sigma}_{ij}^{\theta}(x,t)$ denotes the linear elastic solution of pure thermal load $\theta(x,t)$, λ_θ and λ_P are thermal load multiplier and mechanical load multiplier respectively. Suppose the Drucker's theorem is satisfied for structural material, the stress and strain rate in a typical time cycle under cyclic loads gradually reaches the steady-state:

$$\sigma_{ij}(t) = \sigma_{ij}(t+\Delta t) \tag{2}$$

$$\dot{\varepsilon}_{ij}(t) = \dot{\varepsilon}_{ij}(t+\Delta t) \tag{3}$$

For arbitrary cyclic history, the stress solution $\sigma_{ij}(x,t)$ is given by:

$$\sigma_{ij}(x,t) = \lambda \hat{\sigma}_{ij}(x,t) + \bar{\rho}_{ij}(x) + \rho_{ij}^{r}(x,t) \tag{4}$$

where λ is the load multiplier, $\bar{\rho}_{ij}(x)$ is a constant residual stress field; $\rho_{ij}^{r}(x,t)$ is a varying residual stress field in each cycle, which satisfies:

$$\rho_{ij}^{r}(x,0) = \rho_{ij}^{r}(x,\Delta t) \tag{5}$$

2.2 The global minimization process for shakedown analysis

The LMM strict shakedown analysis scheme in this paper is based on the Koiter upper bound shakedown theorem, the solution of shakedown limit multiplier involves a process of energy minimization, which is given by incremental formulation:

$$I(\Delta\varepsilon_{ij}^{n},\lambda) = \sum_{n=1}^{N} \int_V \left[\sigma_{ij}^{n}\Delta\varepsilon_{ij}^{n} - \left(\lambda\hat{\sigma}_{ij}(t_n) + \bar{\rho}_{ij} + \rho_{ij}^{r}(t_n)\right)\Delta\varepsilon_{ij}^{n}\right] dV \tag{6}$$

$$\rho_{ij}^{r}(t_n) = \sum_{l=1}^{n} \Delta\rho_{ij}^{r}(t_l) \tag{7}$$

where $\Delta\varepsilon_{ij}^{n}$ denotes the strain increment at load instance $n(n = 1 \sim N)$; N is the number of load instances in each cycle. The minimization of $I(\Delta\varepsilon_{ij}^{n},\lambda)$ requires that the sum of plastic strain increments in one cycle satisfies the strain compatibility condition. Suppose a series of plastic strain increments $\Delta\varepsilon_{ij}^{nk}$ are known at the k th iteration, a linear elastic material with shear modulus $\bar{\mu}^{nk}$ can be defined to make the stress state of the structure reach the yield surface under the same strain condition:

$$\frac{3}{2}\bar{\mu}^{nk}\bar{\varepsilon}(\Delta\varepsilon_{ij}^{nk}) = \sigma_y \tag{8}$$

where $\bar{\varepsilon} = \sqrt{\frac{2}{3}\Delta\varepsilon_{ij}^{nk}\Delta\varepsilon_{ij}^{nk}}$, denotes the von Mises equivalent strain.

For shakedown analysis, there is only a constant residual stress term $\bar{\rho}_{ij}$, and the varying residual stress field in a cycle remains zero $\rho_{ij}^{r} = 0$. Therefore, the cyclic stress history of shakedown problem can be expressed as:

$$\sigma_{ij}(x,t) = \lambda\hat{\sigma}_{ij}(x,t) + \bar{\rho}_{ij}(x) \tag{9}$$

A series of linear incremental relationships can be defined as:

$$\Delta\varepsilon_{ij}^{n(k+1)'} = \frac{1}{2\bar{\mu}^{nk}}\left[\lambda\hat{\sigma}'_{ij}(t_n) + \bar{\rho}_{ij}^{k+1'}\right] \tag{10}$$

where the superscript $'$ indicates deviatoric variables. By adding the linear increment expressions over a cycle, we can get:

$$\Delta\varepsilon_{ij}^{(k+1)'} = \sum_n \Delta\varepsilon_{ij}^{n(k+1)'} = \frac{1}{2\bar{\mu}^{k}}\left[\lambda\sigma_{ij}^{in'} + \bar{\rho}_{ij}^{k+1'}\right] \tag{11}$$

where $\Delta\varepsilon_{ij}^{(k+1)} = \sum_n \Delta\varepsilon_{ij}^{n(k+1)}$ is the summation of strain increment in a cycle, and meets the strain coordination condition; $\bar{\mu}^{k}$ is calculated by $\frac{1}{\bar{\mu}^{k}} = \sum_n \frac{1}{\bar{\mu}^{nk}}$; σ_{ij}^{in} is calculated by $\sigma_{ij}^{in} = \bar{\mu}^{k}\sum_n \frac{\lambda\hat{\sigma}_{ij}(t_n)}{\bar{\mu}^{nk}}$. After a number of iterations with (11), the minimization of $I(\Delta\varepsilon_{ij}^{n},\lambda)$ is reached, where $I(\Delta\varepsilon_{ij}^{n(k+1)},\lambda) \leq I(\Delta\varepsilon_{ij}^{n(k)},\lambda)$.

2.3 Shakedown limit multiplier

The shakedown limit multiplier can be calculated based on the upper-bound theorem as follows:

$$\lambda^{S} = \frac{\int_V\left(\sum_{n=1}^{N}\sigma_{ij}^{n}\Delta\varepsilon_{ij}^{n}\right)dV}{\int_V\left(\sum_{n=1}^{N}\hat{\sigma}_{ij}(t_n)\Delta\varepsilon_{ij}^{n}\right)dV} = \frac{\int_V\left(\sigma_y\sum_{n=1}^{N}\bar{\varepsilon}\left(\Delta\varepsilon_{ij}^{n}\right)\right)dV}{\int_V\left(\sum_{n=1}^{N}\hat{\sigma}_{ij}(t_n)\Delta\varepsilon_{ij}^{n}\right)dV} \tag{12}$$

A series of monotonically decreasing load multipliers can be derived using (12), which approach to the actual shakedown limit.

The above LMM procedure for elastic shakedown analysis has been implemented in ABAQUS[26] using user subroutines. It is worth noting that for the plane stress analysis in this paper, the stress tensor and strain tensor in ABAQUS reduced to three components respectively.

3. Two-plane model

In order to obtain different kinds of elastic shakedown boundaries under the interaction of mechanical membrane stress, thermal bending stress and thermal membrane stress, the two-plane model proposed in literature[7] is adopted. The schematic diagram of the model is shown in Fig.1. The analysis of this paper adopts the assumption of section translation deformation, and the interaction of primary bending stress with the above three types of stresses will be discussed in a separate paper.

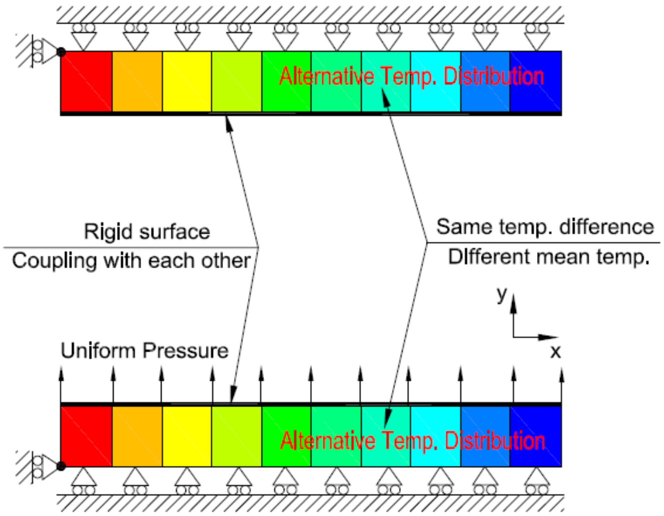

Fig. 1. Two-plane FE model.

The two-plane model consists of two identical plane stress models. The two planes are rigidly coupled by two inner adjacent edges, and the two outside boundary lines are restrained in *Y*-direction. The total bending strain of the section is constrained to zero, rigid boundary subjected to mechanical load is set parallel to the fixed boundary. The uniform primary membrane stress can be obtained by directly applying the mechanical load on the coupling boundary. Note that mechanical loads are beard by two planes together because of the coupling condition. The uniform distribution thermal membrane stress and the linear distribution thermal bending stress can be achieved by designing the temperature field applied on the two planes. As shown in Fig. 1, the two planes are respectively applied with linearly distributed temperature gradients in the *X* direction, and the gradient distribution of the temperature field is represented by different color blocks. The two planes have the same temperature gradient range but with different mean temperatures. The thermal bending stress is induced by the temperature gradient, the maximum linear elastic thermal bending stress caused by the thermal gradient in the model is $\sigma_{sb}=E\alpha\Delta T/2$, where E is Young's modulus, α is thermal expansion coefficient, and $\triangle T$ is the range of temperature gradient applied to each plane. The thermal membrane stress is caused by the average temperature of the two planes. Assume $\sigma_{sm}=R\sigma_{sb}$, where $R\geq 0$, defined as "secondary membrane bending ratio", is a new parameter introduced in this paper.

Commercial FE software ABAQUS is used for LMM analysis and calculation. The mesh and geometric dimensions of the model are shown in Fig. 2. The properties of elastic-perfectly plastic material are shown in Table 1. It is assumed that the material parameters are constant during the temperature cycles. A homogeneous, isotropic material model with small displacement theory shall be utilized in the analysis. The von Mises yield function and associated flow rule are assumed. There are 180 plane stress elements in the model. The element type is CPS8, and each element has 3 × 3 Gauss integral points.

According to the linear elastic superposition analysis of three types of stresses under uniaxial stress state, the maximum stress in the model will appear at the edge of the structure. As the existing studies[27] have shown that the accurate determination of the alternating plastic boundary is sensitive to the mesh size, so a denser mesh is utilized at the edge of the model. The following calculation results show that sufficiently accurate shakedown limit multiplier can be obtained by using the mesh.

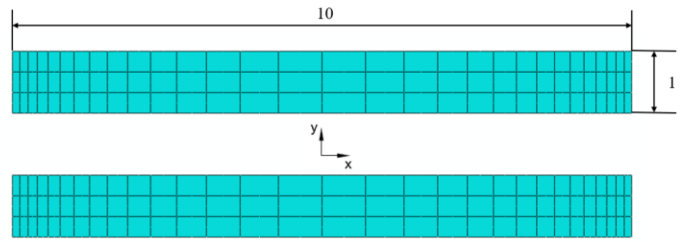

Fig. 2. Meshing and dimensions of geometry.

Table 1. Material property.

Item	Value
Young's modulus [MPa]	2E5
Poisson's ratio	0.3
Yield strength [MPa]	300
Coefficient of thermal expansion [°C^{-1}]	1E-5

4. Shakedown analysis of modified Bree problems

Three types of cyclic loading forms are considered in this paper and shown in Fig. 3.

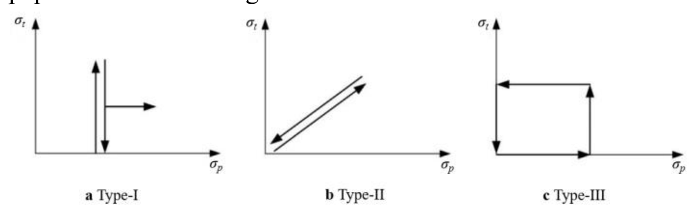

Fig. 3. Three loading forms of modified Bree shakedown problems.

4.1 Type-I loading form

For the Type-I loading case, the thermal load is cyclic and the mechanical load remains constant, as shown in Fig. 3a. Note that constant mechanical load can cause constant mechanical membrane stress, while cyclic thermal bending stress and cyclic thermal membrane stress are both induced by the cyclic thermal load. In order to quantitatively analyze the respective proportions of thermal membrane stress and thermal bending stress in thermal stress, and to distinguish their influence on shakedown boundary, the concept of "secondary membrane bending ratio" is introduced, which is expressed as R:

$$R = S_{Qm}/S_{Qb} = \sigma_{sm}/\sigma_{sb} \tag{13}$$

where S_{Qm} is the thermal membrane stress range, S_{Qb} is the thermal bending stress range. The secondary equivalent thermal stress range can be expressed as:

$$S_{Qmb} = S_{Qm} + S_{Qb} = \sigma_t - 0 = \lambda^S \lambda_\theta \sigma_{t0} \tag{14}$$

where σ_{t0} is the maximum absolute value of the thermal stress obtained by applying the elastic analysis method according to the initial preset temperature field. As noted by literature[4], pure thermal bending can be induced by linear distribution thermal gradient in radial direction of the shell, while the axial thermal gradient will cause both thermal membrane and thermal bending, with membrane being dominant. Although the source and stress distribution of the two are different, the cyclic properties of the two are the same, and both are part of the cyclic thermal stress caused by the cyclic thermal load. The secondary membrane plus bending stress ranges should be both subtracted from the cyclic yield stress in the non-cyclic derivation. Therefore, when solving the shakedown limit multiplier, the thermal membrane and thermal bending are scaled according to the same load multiplier. Different thermal stress distribution forms are reflected by different R values. For example R=0 represents pure thermal bending; $1/R=\sigma_{sb}/\sigma_{sm}=0$ means pure thermal membrane; R=0.5, then $\sigma_{sm}=0.5\sigma_{sb}$. The introduction of R can make the three-dimensional shakedown boundary expressed in the form of parameterized lines in the two-dimensional coordinate system instead of the usual contour lines. It is convenient for comparison and reduces unnecessary simplification. A series of R values (0, $\frac{1}{9}$, $\frac{1}{4}$, $\frac{3}{7}$, $\frac{2}{3}$, $\frac{4}{5}$, 1, $\frac{3}{2}$, $\frac{7}{3}$, 4, 9, + (represents pure thermal membrane)) are selected for calculation and analysis to study the change of shakedown region under different thermal stress distributions. According to the non-cyclic derivation[4], the corresponding three-dimensional elastic shakedown boundary section under constant mechanical membrane stress and cyclic thermal stress can be expressed as:

Case a. for $S_{Qb}+S_{Qm} \le 2S_y$, and $S_{Qm} \ge S_{Qb}$

$$X = 1 - Z/2 \tag{15}$$

Case b. for $S_{Qb}+S_{Qm} \le 2S_y$, and $S_{Qm} \le S_{Qb}$

$$X = 1 - Y/4 - Z^2/4Y \tag{16}$$

where $X = P_m/S_y$, P_m is the general primary membrane equivalent stress, S_y is the cyclic yield strength. $Y=S_{Qb}/S_y$, $Z=S_{Qm}/S_y$. By introducing the parameter R, it can be derived from Eqs. (15) and (16) that:

when $Y' \le 2$ and $R \ge 1$:

$$Y' = S_{Qmb}/S_y = 2(1+1/R)(1-X) \tag{17}$$

when $Y' \le 2$ and $0 \le R \le 1$:

$$Y' = 4(1-X)(1+R)/(1+R^2) \tag{18}$$

The LMM was implemented to perform strict shakedown analysis of the model under various ratios of R. A convergence value of 1e-4 between consecutive upper bounds was used to obtain the shakedown limits. The numerical results are shown in Fig. 4 and Fig. 5. Fig.4 shows comparison between the shakedown limits calculated by the LMM and the theoretical solutions directly obtained from Eqs. (17) and (18). It can be seen that the numerical solution is in good agreement with the theoretical solution. As shown in Fig.5, except for the case of pure thermal membrane, the shakedown boundary under different R is composed of two segments. One of which is the alternating plastic boundary, and the other is the ratcheting boundary. When R=0, i.e. the thermal stress is pure thermal bending, the governing equations of the shakedown boundary can be obtained from Bree diagram as follows：

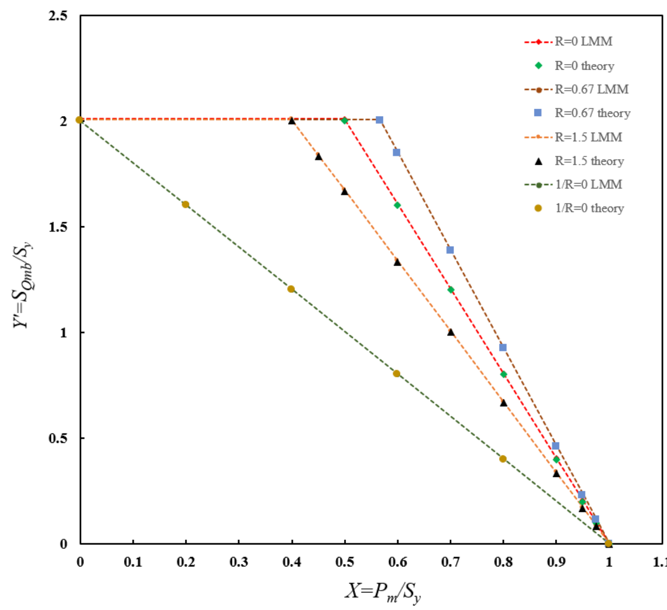

Fig. 4. Comparison of partial shakedown limits calculated by the LMM and theoretical solutions.

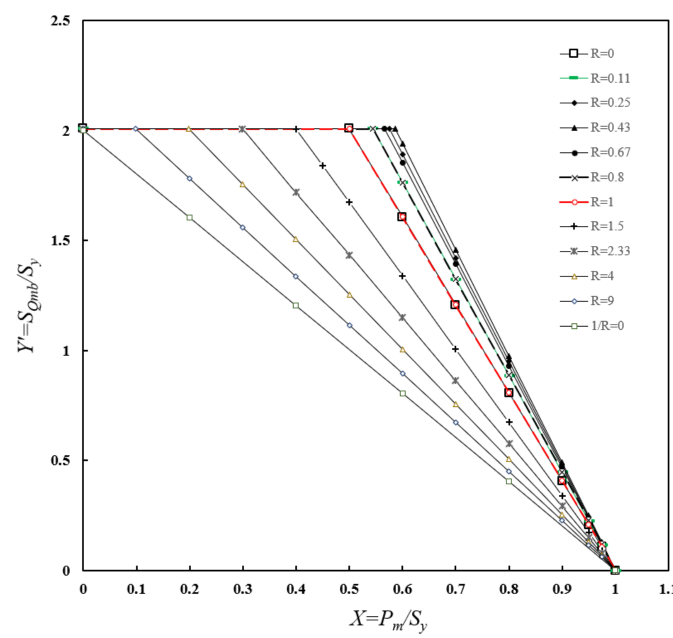

Fig. 5. Shakedown limits calculated by the LMM for the Type-I loading case.

$$Y' = Y = 2 \quad \text{for} \quad 0 \le X \le 0.5 \tag{19}$$

$$Y' = Y = 4(1-X) \quad \text{for} \quad 0.5 < X \le 1.0 \tag{20}$$

For different values of R, the alternating plastic boundary always remains unchanged, that is, the secondary equivalent thermal stress range is equal to twice the yield strength. When R=1, the ratcheting boundary section (hereinafter referred to as lower shakedown boundary) is the same as that when R=0, that is,

$Y' = 4(1 - X)$. In Fig.5, the red dotted line is the shakedown boundary for R=1. When R>1, the lower shakedown boundaries are all on the left side of the red dotted line, When R<1 , the lower shakedown boundaries are all located to the right of the red dotted line. It can be seen that with the change of R, the intersection point of the alternating plastic boundary and the lower shakedown boundary is always changing, thus affecting the area of the shakedown region. Here, we define the abscissa value of the intersection point as the critical value [X]. When Y'=2, formula (21) is obtained from Eqs. (17) and (18).

$$[X] = \begin{cases} 1/(1+R), & \text{for } R \geq 1 \\ (1+2R-R^2)/2(1+R), & \text{for } 0 \leq R \leq 1 \end{cases} \tag{21}$$

When R≥1, the critical value [X] decreases as R increases. It means that the shakedown region decreases with the increase of the proportion of thermal membrane in thermal stress. When the thermal stress is pure thermal membrane, the shakedown region reaches the minimum and the shakedown boundary is controlled by a single straight line. When $0 \leq R \leq 1$, the critical value[X] first gradually increases as R increases, and then gradually decreases. When R=$\sqrt{2}$-1, [X] achieves the maximum value, and $[X]_{\max}$=2-$\sqrt{2}$ ≈0.586. In Fig. 6, all numerical results in Fig. 5 are plotted in the same coordinate system as the Bree diagram. The ordinate is the dimensionless thermal bending stress range. From Fig. 6, we can see the changing trend of the critical value [X]. As the R value increases, the shakedown zone corresponding to thermal bending gradually decreases.

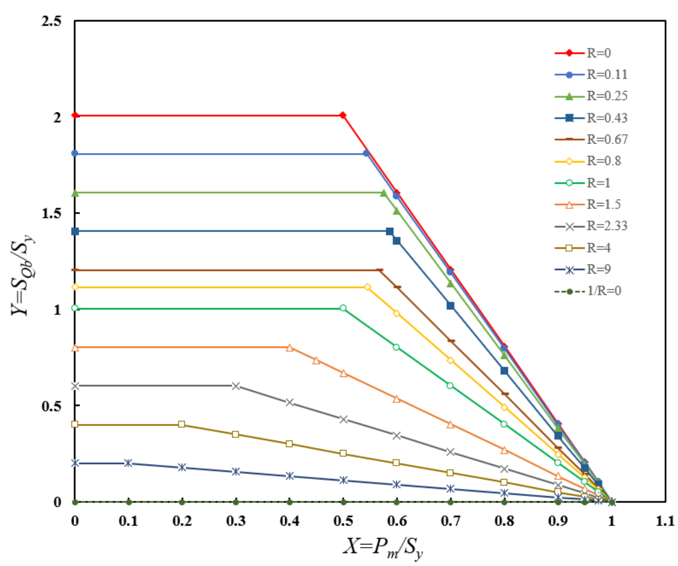

Fig. 6. Shakedown limits plotted in the *XY* coordinate system.

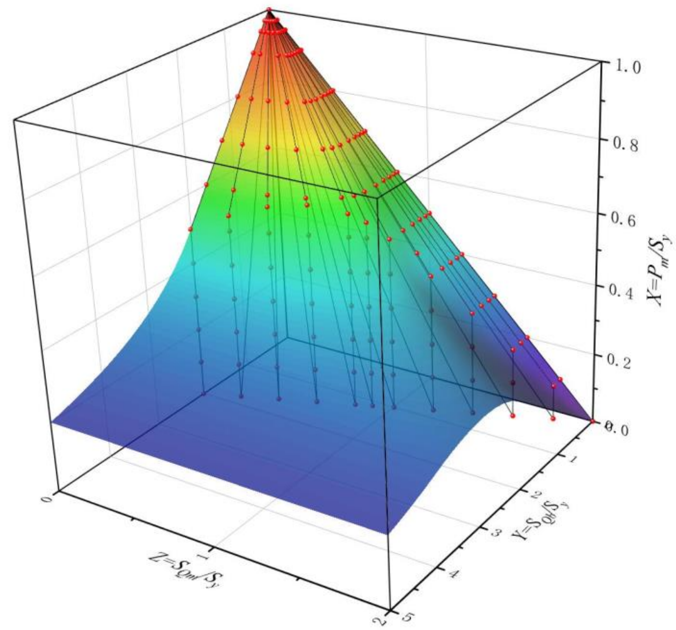

Fig. 7. Shakedown limits plotted in the *XYZ* coordinate system and its locations in the Reinhardt 3D ratcheting boundary.

In Fig.7, the calculated shakedown limits (the red dots) are displayed in the three-dimensional *XYZ* coordinate system. The locations of the shakedown limits on and below the colored Reinhardt three-dimensional ratcheting boundary[4] are marked. The relative positional relationship between the three-dimensional shakedown domain and ratcheting boundary is presented. The complete elastic shakedown boundary under Type-I loading case can be expressed as Eqs. (22) and (23):

when R≥1 :

$$Y' = \begin{cases} 2, & 0 \leq X \leq [X] \\ 2(1+1/R)(1-X), & [X] \leq X \leq 1 \end{cases} \tag{22}$$

when $0 \leq R \leq 1$:

$$Y' = \begin{cases} 2, & 0 \leq X \leq [X] \\ 4(1-X)(1+R)/(1+R^2), & [X] \leq X \leq 1 \end{cases} \tag{23}$$

where $[X]$ is determined by Eq. (21). Since the elastic shakedown boundary always passes through two fixed points (1,0) and (0,2) in the XY' coordinate system, so once the critical value $[X]$ is determined, the elastic shakedown domain can be quickly constructed.

4.2 Type-II loading form

For the Type-II loading case, the thermal load and the mechanical load vary proportionally, i.e. the primary load cycling in-phase with the secondary load, as shown in Fig. 3b. Bradford[9] theoretically deduced the modified Bree problem that both the primary load and the secondary load are strictly in-phase cycle. The governing equation of Bradford shakedown boundary represented by the black dotted line in Fig.8 can be expressed as:

$$X'+Y = 2 \quad \text{for } 0 \leq X' \leq 1 \tag{24}$$

where X'=$\triangle P_m/S_y$, and $\triangle P_m$ is the primary membrane stress range. In Bradford's work, the thermal stress is purely thermal bending stress as the Bree problem, that is, R=0, without considering the effect of thermal membrane stress. In this section, the elastic shakedown behavior under the same in-phase cycle of thermal bending stress, thermal membrane stress and mechanical membrane stress is considered, i.e. R≥0. When R=0, the calculated shakedown limits agree well with the Bradford theoretical solution. When the R value is arbitrarily changed, the shakedown boundary always remains unchanged in the $X'Y'$ coordinate system. Therefore, it can be summarized that the elastic shakedown boundary governing equation under Type-II loading condition is as follows:

when R≥0 :

$$X'+Y' = 2 \quad \text{for } 0 \leq X' \leq 1 \tag{25}$$

Note the change of the ordinate variable in (25).

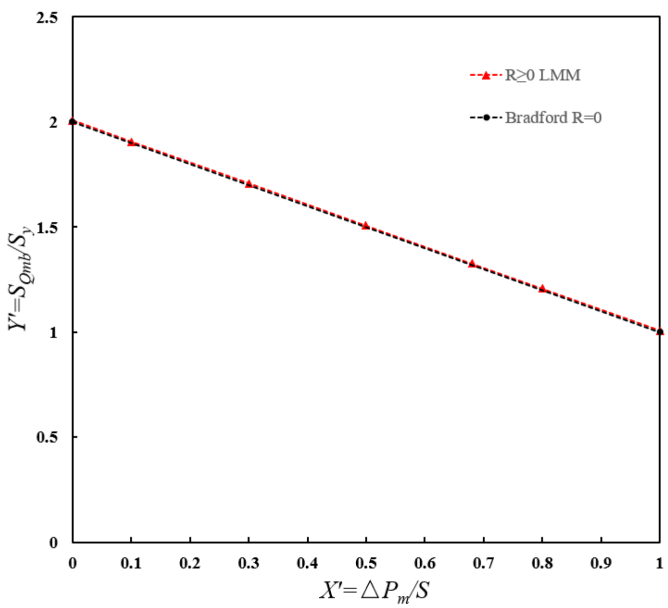

Fig. 8. Shakedown limits calculated by the LMM for the Type-II loading case and its comparison with the Bradford shakedown boundary.

The following is an analysis of why the shakedown boundary remains unchanged after considering the thermal membrane stress in the thermal stress. For the case of in-phase loading, the constant loading part is zero, and all loadings are cyclic. In order to maintain elastic shakedown and to protect against fatigue failure, the sum of the maximum stress range caused by all loadings shall not exceed twice the yield stress, i.e.

$$\triangle P_m + S_{Qm} + S_{Qb} \leq 2S_y \tag{26}$$

Divide both sides of InEq. (26) by S_y, then, X'+Y+Z≤ 2, that is, X'+Y' ≤ 2. Since it is the maximum stress ranges of primary stress plus secondary stress on the entire wall thickness that control the shakedown boundary, the actual ratio of thermal membrane and thermal bending has no effect on the shakedown boundary.

4.3 Type-III loading form

For the Type-III loading case, the thermal load and the mechanical load vary independently, as shown in Fig. 3c. The numerical results calculated by the LMM are shown in Fig.9. As the value of R continues to increase, the changing trend of the shakedown domain for Type-III loading is similar to that of the Type-I loading. Besides pure thermal membrane, the shakedown boundary consists of two segments. The alternating plastic boundary segment is the same as the Type-II loading case. The lower shakedown boundary coincides with the corresponding boundary segment of the Type-I loading. In fact, by summarizing and comparing the three types of modified Bree shakedown problems, it can be found that the shakedown boundary of the Type-III loading case is always the lower envelope of the shakedown boundaries of the Type-I loading case and the Type-II loading case for any selected R value.

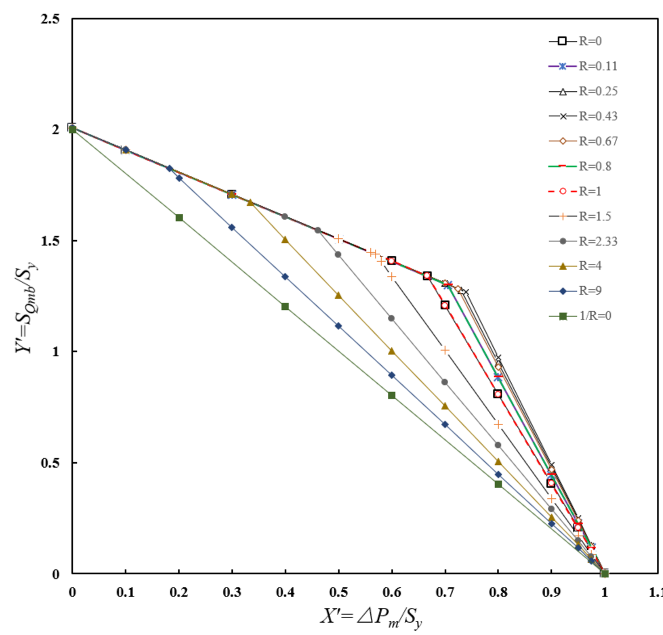

Fig. 9. Shakedown limits calculated by the LMM for the Type-III loading case.

As shown in Fig.10, several typical R values are selected to summarize the calculation results of shakedown limits for the three types of modified Bree problems. Based on the first two types of problems, the governing equations of the shakedown boundary under the Type-III loading can be obtained as:

when R≥1:

$$Y' = \begin{cases} 2 - X', & 0 \leq X' \leq [X'] \\ 2(1 + 1/R)(1 - X'), & [X'] \leq X' \leq 1 \end{cases} \tag{27}$$

when 0 ≤R≤ 1:

$$Y' = \begin{cases} 2 - X', & 0 \leq X' \leq [X'] \\ 4(1 - X')(1 + R)/(1 + R^2), & [X'] \leq X' \leq 1 \end{cases} \tag{28}$$

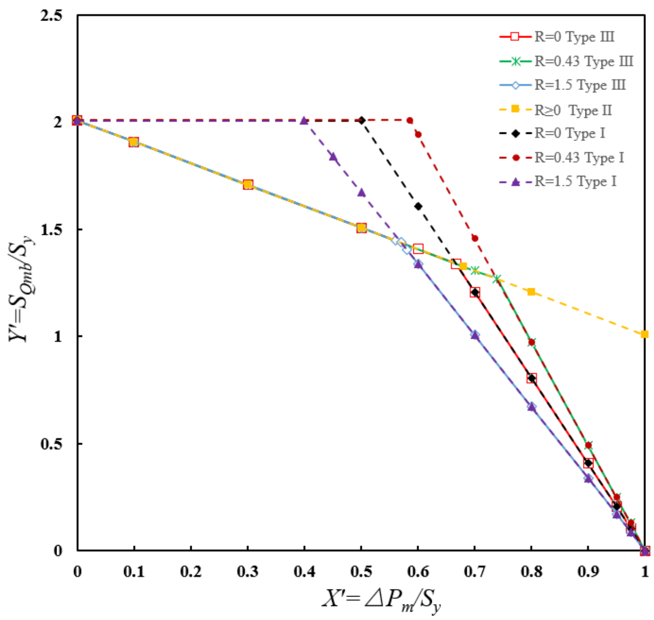

Fig. 10. Comparison of the shakedown boundaries for the three types of modified Bree problems.

where the abscissa $[X']$ of the inflection point of the shakedown boundary is determined by Eq. (29).

$$[X'] = \begin{cases} 2/(2+R), & R \geq 1 \\ (2+4R-2R^2)/(3+4R-R^2), & 0 \leq R \leq 1 \end{cases} \tag{29}$$

For $R \geq 0$, $[X']$ first increases and then decreases with the increase of R value. When $R=\sqrt{2}$-1, $[X']$reaches the maximum, and $[X']_{max}$= $(4\sqrt{2}$-4)/(3$\sqrt{2}$-2) ≈0.739. Through the comparison of the three types of modified Bree shakedown problems, it can be found that different thermal stress distributions (reflected by different R values) have a great impact on the area of the shakedown region. An optimized temperature field design can expand the scope of the shakedown region and improve the economy.

5. Complete elastic shakedown assessment method

The 3S criterion (also known as shakedown criterion or twice yield criterion) is the elastic ratcheting analysis method in the ASME code that can be used for elastic shakedown analysis. However, the question of whether 3S criterion can guarantee shakedown and protect against ratcheting has long been discussed internationally. ISO 16528 Standard[28] states that the 3S criterion covers the risk of failure by progressive plastic deformation. Zeman pointed out 3S-criterion based on elastic shakedown concepts is a necessary but not sufficient condition for shakedown to linear-elastic behavior [29].

According to the definition of 3S criterion, it can be expressed as:

$$\Delta P + \Delta Q \leq 3S \tag{30}$$

where ΔP is the primary stress range, ΔQ is the secondary stress range. InEq. (30) divided by S_y, the 3S criterion can be expressed in a dimensionless form as:

$$X' + Y' \leq 2 \tag{31}$$

For the Type-I loading condition, as the mechanical load P is constant, then ΔP=0, that is, X'=0, and the 3S criterion becomes $Y' \leq 2$. For the Type-II and Type-III loading conditions, since both the primary load and the secondary load are cyclic, the 3S criterion can be expressed by Eq. (31). Fig.11 to Fig.13 are the comparisons of the three-dimensional shakedown domains and the 3S criterion plane of the three types of problems. (Fig.11 is plotted in the XYZ coordinate system, Fig.12 and Fig.13 are plotted in the $X'YZ$ coordinate system). The blue surfaces in Fig.11 and Fig.13 are the three-dimensional shakedown boundaries, and the green planes are the 3S criterion planes. Part of the area where the 3S criterion plane and the shakedown domain overlap are shown in blue. In Fig.12, the blue plane is the three-dimensional shakedown boundary, and the 3S criterion plane coincides with this plane. The blue dots in Fig.13 are the inflection points of the shakedown boundary under different R values, which are all located on the 3S criterion plane.

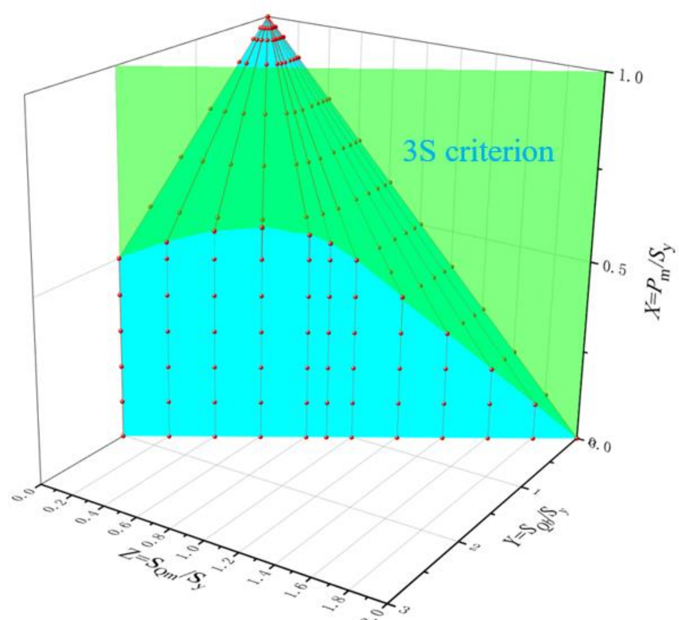

Fig. 11. Comparison between shakedown domain for the modified Bree problem under Type-I loading and the 3S criterion plane.

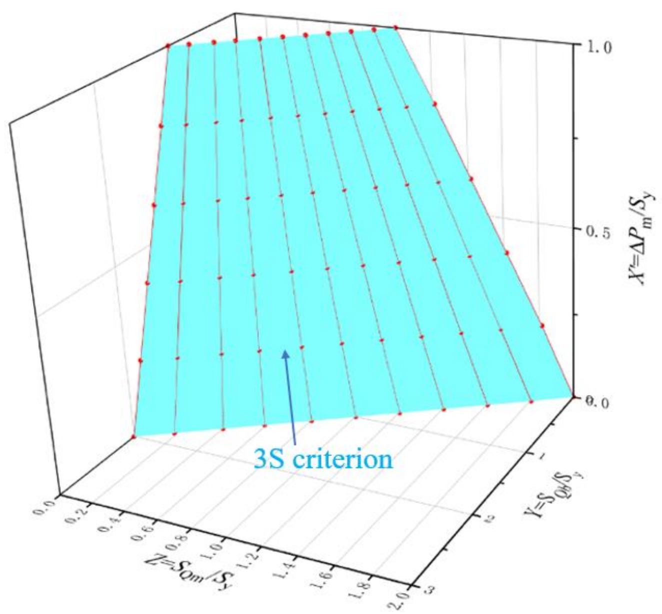

Fig. 12. Shakedown domain and 3S criterion plane for the modified Bree problem under Type-II loading.

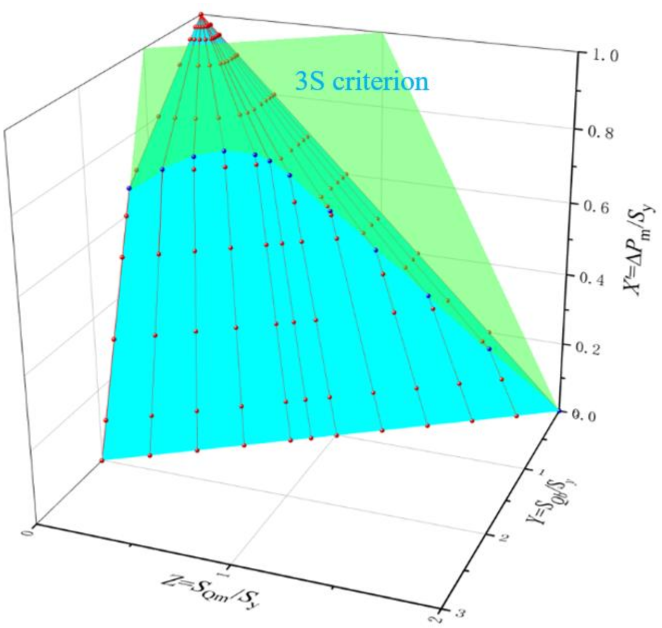

Fig. 13. Comparison between shakedown domain for the modified Bree problem under Type-III loading and the 3S criterion plane.

From Fig.11 to Fig.13, it can be seen that the 3S criterion does not represent a complete elastic shakedown boundary except for specific loading case. This is the source of the non-conservatism of the 3S criterion used for elastic ratcheting analysis. In order to eliminate this incompleteness, additional assessment conditions need to be supplemented. For the Type-I loading, the 3S criterion is conservative when $X < [X]$(that is given by Eq. (21)). When $X > [X]$, the 3S criterion plane exceeds the lower shakedown boundary that can be determined by the second formulas in Eqs. (22) and (23). As for the Type-II loading, the 3S criterion is a sufficient and necessary condition for shakedown assessment, and is conservative in the whole interval of X'.

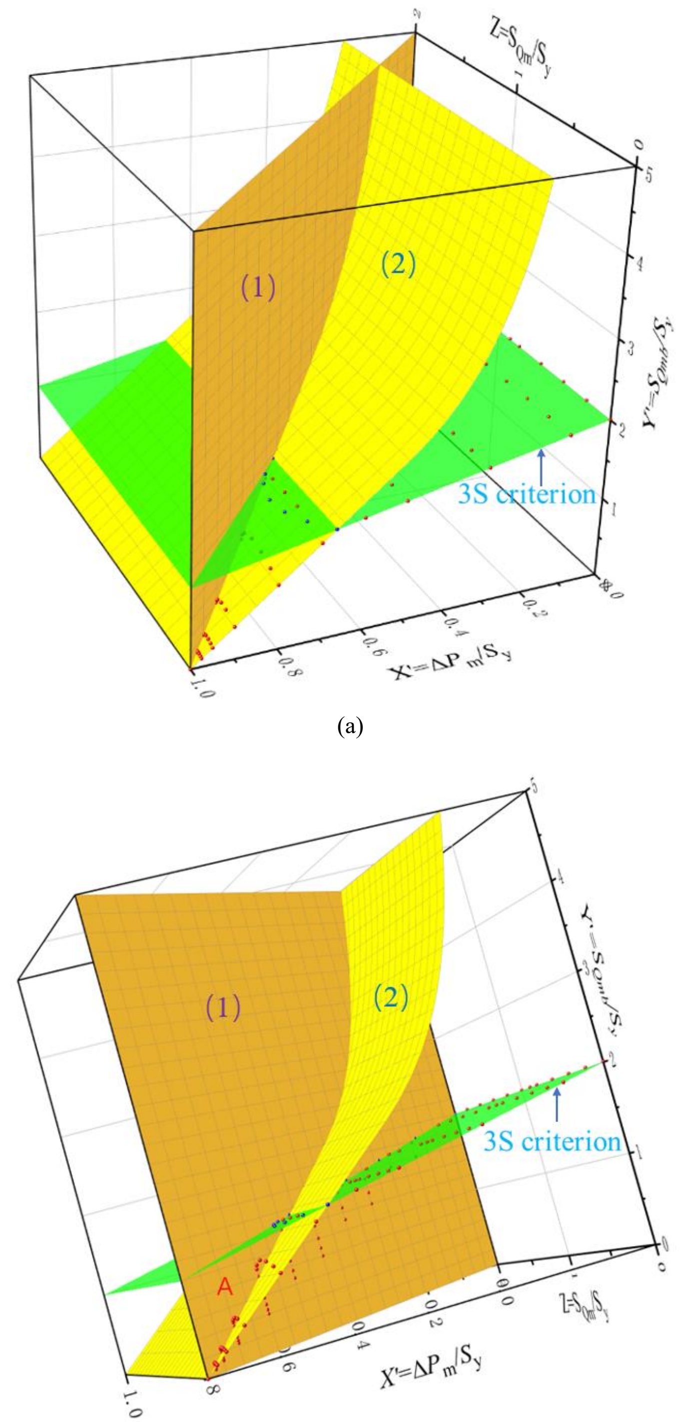

Fig. 14. Shakedown limits for the modified Bree problem under Type-III loading displayed in the $X'Y'Z$ coordinate system and its comparison with the 3S criterion plane.

For the Type-III loading, the shakedown domain is more conservative than that of Type-I loading and Type-II loading. Fig.14 compares the shakedown limits for the Type-III problem with the 3S criterion plane in the $X'Y'Z$ coordinate system. The green plane is the 3S criterion plane. The orange plane (1) and the yellow surface (2) are the checking surfaces of thermal stress ratcheting, and they can be used to show the positions of the shakedown limits in space. The shakedown limits lie partly on the green plane, partly on the orange plane, and the rest locate below the green plane and above the yellow plane. If the 3S criterion is supplemented with the orange and yellow planes, the elastic shakedown can be ensured to protect against ratcheting. The three-dimensional elastic shakedown boundary given by these three surface constraints can be uniformly expressed as:

$$X' = F(Y', Z) = \min\left\{\begin{bmatrix} 1 - Y'/4 \text{ if } Y' \leq 4/3 \\ 2 - Y' \quad \text{if } Y' > 4/3 \end{bmatrix}, (2 - Z)/2\right\} \quad (32)$$

In the region A surrounded by the three surfaces of Fig. 14(b), the elastic shakedown boundary given by Eq. (32) is more conservative than the actual elastic shakedown limits. Therefore, as a more economical alternative, especially when the primary membrane stress range is greater than S, the 3S criterion can be supplemented by the actual shakedown limits. A new and complete elastic shakedown assessment method for generalized thermomechanical loading conditions can be summarized as follows:

a) Determine the primary membrane stress range to calculate $X'=\triangle P_m \,/\, S_y$.
b) Calculate the secondary equivalent thermal stress range at all locations of interest, $S_{Qmb}= Y'S_y$.
c) Calculate the thermal membrane stress range at all locations of interest, $S_{Qm}= ZS_y$.
d) Determine the secondary membrane bending ratio, $R= S_{Qm} \,/\, (S_{Qmb} - S_{Qm})$, and calculate $[X']$ according to Eq. (29).

Then the elastic shakedown assessment steps are:

(1) When $X' \leq [X']$, the 3S criterion, i.e. $X' + Y' \leq 2$, is conservative.
(2) When $R \geq 1$ and $X' > [X'] = 2/(2+R)$, elastic shakedown assessment based on the 3S criterion alone may lead to progressive plastic deformation. Additional assessment condition should be complemented according to Eq.(27), that is, Z=2$(1-X')$.
(3) When $0 \leq R \leq 1$and $X' > (2+4R-2R^2)/(3+4R-R^2)$, the 3S criterion is not conservative for elastic shakedown evaluation, the second expression of Eq. (28) should be supplemented, that is, $Y' = 4(1-X')(1+R)/(1+R^2)$.

6. Conclusions

Three types of modified Bree shakedown problems involving thermal membrane stress and generalized loading conditions are investigated systematically. To sum up, the following conclusions can be drawn:

1. By introducing a new parameter called "secondary membrane bending ratio" R, the connections between the three types of problems are revealed，and the parametric equations of the three types of shakedown boundaries are obtained for the first time. The proposed parametric equations are useful in engineering optimization design and safety checking.
2. It is found that for the Type-I and Type-III loading conditions, the shakedown domains will first gradually increase and then gradually decrease as the R value increases. For the Type-II loading case, the shakedown boundary coincides with the 3S criterion and remains unchanged under different R values. For any given value of R, the shakedown domain of the Type-III loading is the lower envelope of the shakedown domains of the Type-I loading and the Type-II loading.
3. It is found that the 3S criterion does not represent a complete elastic shakedown boundary except for the case of primary load cycling in-phase with the secondary load. In general, the 3S criterion plane only coincides with the alternating plastic boundary. Due to the lack of the lower shakedown boundary, the 3S criterion is unsafe for elastic shakedown assessment when the primary membrane stress (or range) exceeds its critical value $[X]$ (or $[X']$).
4. A new and complete elastic shakedown assessment method for generalized thermomechanical loading conditions is proposed, which eliminates the incompleteness of the 3S criterion and is a sufficient and necessary condition to prevent the loss of elastic shakedown. Compared with the three-dimensional elastic ratcheting assessment method proposed based on the ASME code rule, it is a more economical alternative, especially when there exists local primary membrane stress.

Acknowledgment

The authors are grateful for the supports provided by the National Key Research and Development Program of China (Grant No. 2017YFF0210704) and the National Natural Science Foundation of China (Grant No. 11672147).

References

[1] J. Bree, Elastic-plastic behavior of thin tubes subjected to internal pressure and intermittent high-heat fluxes with application to fast-nuclear-reactor fuel elements. J. Strain Anal. 2.3 (1967): 226-238.
[2] J. Bree, Incremental growth due to creep and plastic yielding of thin tubes subjected to internal pressure and cyclic thermal stresses, J. Strain Anal. 3 (1968):122–127.
[3] A. Kalnins, Presentation at the Meeting of the ASME BPVC Subgroup Design Analysis, Minutes of the Subgroup Design Analysis, in:, March 2005.

[4] W. Reinhardt, On the Interaction of Thermal Membrane and Thermal Bending Stress in Shakedown Analysis[C]// ASME Pressure Vessels & Piping Conference. 2008.
[5] ASME Boiler & Pressure Vessel Coe, VIII Division 2 Alternative Rules, Rules for Construction of Pressure Vessels, 2013.
[6] A. Asadkarami, W. Reinhardt, Shakedown at Thermal Discontinuities Involving Thermal Membrane and Thermal Bending Stress[C]// ASME Pressure Vessels & Piping Conference. 2012:433.
[7] J. Shen, H.F. Chen, Y. Liu, A new four-dimensional ratcheting boundary: derivation and numerical validation. European Journal of Mechanics - A/Solids, 71(2018) 101-112.
[8] D. Moreton, H. Ng, The extension and verification of the Bree diagram, in: Structural Mechanics in Reactor Technology, L, 1981.
[9] R.A.W. Bradford, The Bree problem with primary load cycling in-phase with the secondary load, Int. J. Pres. Ves. Pip. 99–100 (2012) 44–50.
[10] R.A.W. Bradford, The Bree problem with primary load cycling out-of-phase with the secondary load, Int. J. Pres. Ves. Pip. 154 (2017) 83–94.
[11] D.W. Spring, C. Panzarella, D.A. Osage, Revisiting the Bree diagram, in: ASME 2016 Pressure Vessels and Piping Conference, American Society of Mechanical Engineers, 2016.
[12] X. Pei, P. Dong, A universal approach to ratcheting problems of Bree type incorporating arbitrary loading and material nonlinearity conditions. Int. J. Pres. Ves. Pip, 185 (2020) 104137.
[13] X. Pei, P. Dong, J. Mei, The effects of kinematic hardening on thermal ratcheting and Bree diagram boundaries. Thin-Walled Structures, 159 (2021) 107235.
[14] H. Peng, Y. Liu, H.F. Chen, et al. Shakedown analysis of engineering structures under multiple variable mechanical and thermal loads using the stress compensation method. International Journal of Mechanical Sciences, 140 (2018) 361-375.
[15] ASME Boiler & Pressure Vessel Coe, VIII Division 2 Alternative Rules, Rules for Construction of Pressure Vessels, 2019.
[16] J. Shen, M-W. Lu, H. Bao, et al. A modification on 3S criterion and simplified elastic-plastic ratcheting analysis in ASME VIII-2. Int. J. Pres. Ves. Pip. 188 (2020) 104215.
[17] H. W. Ng, D. N. Moreton, Bree diagrams for alternative loading sequences. Engineering approaches to high temperature design(A 84-37877 17-39). Swansea, Wales, Pineridge Press, 1983: 279-312.
[18] H. W. Ng, D. N. Moreton, Ratchetting rates for a Bree cylinder subjected to in-phase and out-of-phase loading, J. Strain Anal. Eng. Des. 21 (1) (1986) 1–7.
[19] H. W. Ng, D. N. Moreton, Alternating plasticity at the surfaces of a Bree cylinder subjected to in-phase and out-of-phase loading, J. Strain Anal. Eng. Des. 22 (2) (1987) 107–113.
[20] H.F. Chen, Linear matching method for design limits in plasticity． Cmc-Tech Science Press， 20(2) (2010) 159－183．
[21] H.F. Chen , A.R. Ponter, Shakedown and limit analyses for 3-D structures using the linear matching method. Int. J. Pres. Ves. Pip. 78(6) (2001) 443–451.
[22] D. Barbera, H.F. Chen, Y. Liu, et al. Recent developments of the linear matching method framework for structural integrity assessment. J. Pres. Ves. Tech.139(5) (2017) 051101.
[23] H.F. Chen, A.R.S. Ponter, R.A. Ainsworth, The linear matching method applied to the high temperature life integrity of structures. Part 1. Assessments involving constant residual stress fields[J]. Int. J. Pres. Ves. Pip, 83(2) (2006) 123-135.
[24] H.F. Chen, J. Ure, D. Tipping, Integrated structural analysis tool using the Linear Matching Method part 2–Application and verification. Int. J. Pres. Ves. Pip, 120 (2014) 152-161.
[25] H.F. Chen, A.R.S. Ponter, Integrity assessment of a 3D tubeplate using the linear matching method. Part 1. Shakedown, reverse plasticity and ratchetting. Int. J. Pres. Ves. Pip, 82(2) (2005) 85-94.
[26] ABAQUS. Dassault Systems, Version 6.14, 2014.
[27] H. Peng, Y. Liu, H.F. Chen, A numerical formulation and algorithm for limit and shakedown analysis of large-scale elastoplastic structures. Com. Mech, 63(1) (2019) 1-22.
[28] Iso 16528-1, in: Published in Switzerland, 2007, 2007.
[29] J.L. Zeman, F. Rauscher, S. Schindler. Pressure Vessel Design: The Direct Route, Chapter5, Elsevier, 2006, p.71.